Composites Communications 8 (2018) 83–91

Contents lists available at ScienceDirect

Composites Communications

journal homepage: www.elsevier.com/locate/coco

Polyaniline/graphene nanocomposites towards high-performance supercapacitors: A review

Zhaoqi Huang, Le Li, Yufeng Wang, Chao Zhang*, Tianxi Liu

State Key Laboratory for Modification of Chemical Fibers and Polymer Materials & College of Materials Science and Engineering, Donghua University, Shanghai 201620, PR China

ARTICLE INFO

Keywords:
Polyaniline
Graphene
Nanocomposites
Supercapacitor

ABSTRACT

Among frequently investigated advanced electrode materials for supercapacitors, polyaniline (PANI) is considered as an ideal electrode material due to its high theoretical capacitance, desirable chemical stability, easy synthesis and low cost. However, neat PANI electrodes are lack of long-term stability and high power density due to their low surface area, large volume changes during release/doping of ions and low conductivity. The composition of PANI with carbon materials especially conductive and high-surface-area graphene provides an effective approach to solve these problems. This review presents an overview of recent advances in the design, synthesis and applications of PANI/graphene nanocomposites as high-performance electrode materials for supercapacitors. The PANI/graphene nanocomposites can combine the advantages of both electrical double-layer capacitances of graphene and pseudocapacitances of PANI, which therefore exhibit long cycle life and large energy density. Various strategies for the synthesis of PANI/graphene nanocomposites are briefly introduced, and several main factors influencing electrochemical capacitive performances of PANI/graphene nanocomposites are presented and discussed. Finally, the future research directions for the PANI/graphene nanocomposites for supercapacitors are also summarized and discussed.

1. Introduction

Supercapacitors, which possess high power density and prolonged cycle life compared to commercial batteries, play an important role as a promising energy storage system solving the challenging issues of fossil fuel exhaustions and climate changes [1]. Supercapacitors have received considerable attention from both academic and industrial fields because they meet the need of a wide range of energy storage applications requiring short loading cycles with safety and stability such as power backup systems, portable devices, and electric vehicles [2–4]. To overcome the drawbacks of the low energy density of supercapacitors in practical applications, the pursue of electrode materials simultaneously with high energy density and prolonged cycle life are required for boosting energy storage performances in energy storages [5,6].

Supercapacitors can be divided into two types depending on different energy storage mechanisms. One is the electrochemical double-layer capacitors (EDLCs), which store energy by physical adsorption/desorption of ions at interfaces. Conductive and high-surface-area porous carbons are generally ideal electrode materials for EDLCs. The other is the pseudocapacitors that store energy through reversible redox reactions of active materials. The pseudocapacitors can deliver much higher capacitances than that of EDLCs but are greatly limited by poor electrical conductivity and easily damaged structures of the electrodes during cycles.

Conducting polymers are frequently used electrode materials for pseudocapacitors because of their low cost, high conductivity and facile synthesis [7–9]. Conducting polymers especially polyaniline (PANI) show an extremely high theoretical capacitance up to 2000 F g^{-1} [10,11]. However, the electrochemically available active surface of PANI greatly depends on the conductivity of PANI and the diffusion of counter ions, and thus only a small amount of PANI could make contributions to the capacitances [10]. As a result, the experimental values of PANI electrodes are much lower than the theoretical value. Moreover, the PANI species would underwear severe volume changes during cycles, and the cycling stability is also a problem to be solved [12].

The composition of PANI and carbon materials into composite electrode materials has attracted extensive attention due to their superior electrochemical performances by combining the advantages of the electrochemical double-layer capacitances of carbon materials and pseudocapacitances of PANI [8,13,14]. Among various carbon materials, graphene exhibits high conductivity, large surface area, flexibility and excellent chemical stability [15–19]. However, easy aggregations

* Corresponding author.
E-mail address: czhang@dhu.edu.cn (C. Zhang).

https://doi.org/10.1016/j.coco.2017.11.005
Received 11 October 2017; Received in revised form 14 November 2017; Accepted 15 November 2017
Available online 10 April 2018

of graphene lead to decreased surface area and capacitances lower than 200 F g^{-1} as electrode materials [4,20]. In the past few years, the PANI/graphene nanocomposites have emerged as an ideal choice as promising electrode materials. For instances, an exceptionally high capacitance value of 1341 F g^{-1} for a PANI/3D graphene framework in acidic electrolyte has been reported [21]. Reduced graphene oxide (rGO) could induce more expanded coil conformation of PANI chains due to strong π-π stacking between the quinoid rings of PANI and the basal plane of graphene [22]. Enhanced electrical conductivity and buffered volume changes during cycles arising from rGO were also reported for the PANI/graphene nanocomposites [8,23,24]. However, several factors, such as the morphologies, component ratios, PANI doping level of the nanocomposites, as well as the synthesis/fabrication techniques for the nanocomposites, and etc., would definitely influence the electrochemical performances of the PANI/graphene nanocomposites.

In the following, recent advances are presented to give readers an overview of the contemporary status of the PANI/graphene nanocomposites as electrode materials for supercapacitors. The strategies for the synthesis and fabrication of PANI/graphene nanocomposites are summarized, and several factors determining the electrochemical performances of the PANI/graphene nanocomposites are also discussed. Some future directions of the PANI/graphene nanocomposites and problems which need to be solved when compositing PANI with graphene towards high-performance supercapacitors are also proposed.

2. Strategies for the synthesis of PANI/graphene nanocomposites

PANI/graphene nanocomposites can be prepared by different procedures, e.g. simple solution mixing [14,25], layer-by-layer (LbL) assembly [26], chemical oxidative polymerization [27–29], electrochemical oxidative polymerization [13,30,31], and interfacial polymerization [32]. The spatially separated graphene prepared by chemical vapor deposition (CVD) and other physical techniques are less viable due to low yield and high cost, and therefore graphene oxide (GO) with hydrophilic oxygen-containing functional groups prepared by chemical routes are usually used as the starting materials for a sequent composition with PANI [33,34]. Broadly, we have categorized these strategies into self-assembly methods and in-situ polymerization methods, respectively, which will be further discussed in the following. For the self-assembly methods, PANI could be synthesized in advances with unique morphologies, and physical interaction and assembly could be utilized for the synthesis of PANI/graphene nanocomposites [35–37]. For the in-situ polymerization methods, the PANI/graphene nanocomposites could be prepared via chemical or electrochemical oxidative processes involving the in-situ polymerization of PANI on graphene substrates.

2.1. Self-assembly methods

The synthesis of PANI/graphene nanocomposites using the self-assembly methods is predominantly based on the electrostatic interactions between PANI and graphene. Self-assembly is a simple and cost effective method, which could easily construct a nanocomposite structure with a controllable component of PANI and graphene over a wide range. In addition, the self-assembly methods provide the possibility to design diverse morphologies of PANI in advances [42,45,46]. PANI is positively charged in their emeraldine salt form [38], and oppositely, GO carries negative charges due to residual carboxylic groups [39]. Therefore, the efficient dispersion of both PANI and graphene would play key roles in the formation of hierarchical PANI/graphene nanocomposite by diverse processes such as vacuum filtrations [14,40], hydrothermal treatments [41], and solvent evaporations [42].

Strategies for dispersing the two components in aqueous media are crucial for the sequent self-assembly of PANI/graphene nanocomposites [14,43,44]. Water-dispersible PANI nanofibers can be readily obtained through in-situ polymerization of aniline by simply controlling pH without adding any stabilizers [38]. GO sheets can be stably dispersed only in a weak alkaline medium. Choosing a suitable pH value for one component would cause severe aggregations of the other because the acid characteristics of doped PANI restrain the ionization of carboxylic acid and phenolic hydroxyl groups on the GO sheets [39]. To address these issues, Wu et al. synthesized a stable dispersion of PANI nanofibers by dialyzing it to remove excess ions, and this dispersion fascinated further self-assembly process of PANI nanofibers with rGO [14]. Mixing the dispersions of GO and PANI/carbon nanotube (PANI/CNT) (pH = 2.6) would result in coagulations, but after several cycles of washing, the mixture remained quite stable even after one month [40]. The Zeta potentials of the suspensions of PANI and GO were measured to determine the surface charges of PANI and GO in suspensions, and they indicated that the cationic nature of partially doped PANI at pH of 2.5 (Zeta potential = 42 mV) with GO at pH of 3.5 (Zeta potential = -68 mV) were the optimized conditions for building the composite nanostructures of PANI and graphene [36].

A series of PANI/graphene nanocomposites with PANI nanostructures as well as excellent electrochemical performances were fabricated by taking advantages of the self-assembly methods. The PANI/graphene nanocomposites with a nanoscale ordering via LbL assembly have been prepared [26]. Fig. 1 shows the schematic representation of the LbL assembly for the construction of PANI/graphene nanocomposites. The PANI/graphene composite electrodes by the LbL method offered a precise control over the thickness, internal structure and flexibility of the PANI/graphene nanocomposites with enhanced chemical stability and electrical conductivity. The synthesis of a hierarchical film with coaxial CNT@PANI nanocables uniformly sandwiched between

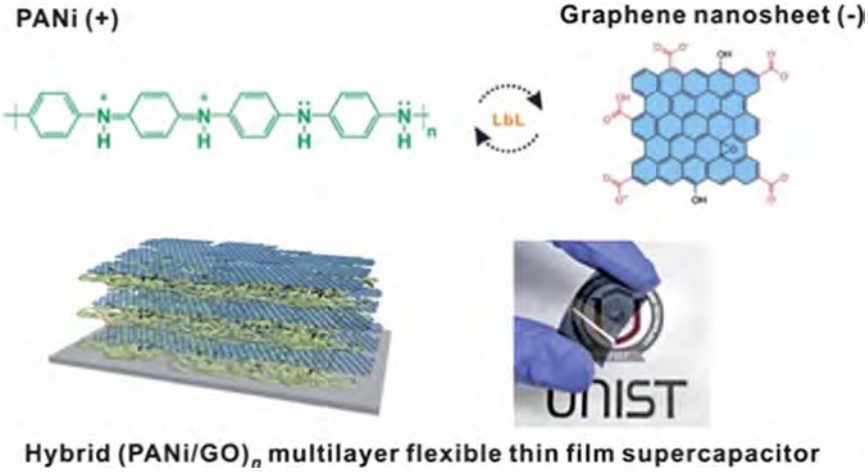

Fig. 1. Schematic representation of LbL assembled multilayer thin film of PANI with GO sheets with a photograph of the film assembled on a flexible PET substrate [26]. Reprinted with permission from Ref. [26], Copyright 2012, the Royal Society of Chemistry.

Table 1
Comparison of the PANI/graphene nanocompsites as supercapacitor electrode.

Electrode materials	Electrolytes	Configurations	Capacitances (F g^{-1})	Capacitance retention, Number of cycles	Ref.
PANI on rGO paper	1 M H_2SO_4	Three electrode	233, 2 mV s^{-1}	100%, 1500	[13]
PANI nanofiber/rGO paper	1 M H_2SO_4	Two electrode	210, 0.3 A g^{-1}	79%, 800	[14]
PANI/rGO	1 M H_2SO_4	Three electrode	1126, 1 mV s^{-1}	84%, 1000	[8]
PANI/rGO	1 M H_2SO_4	Three electrode	746, 0.2 A g^{-1}	78%, 500	[90]
CNT@PANI/rGO paper	1 M HCl	Three electrode	569, 0.1 A g^{-1}	96%, 5000	[40]
PANI/rGO film	1 M H_2SO_4	Three electrode	640, 0.1 A g^{-1}	90%, 1000	[45]
PANI/sulfonated rGO	1 M H_2SO_4	Three electrode	763, 5 mV s^{-1}	85%, 1000	[32]
LbL-assembled PANI/rGO	1 M H_2SO_4	Three electrode	375, 0.5 A g^{-1}	90%, 500	[26]
PANI nanorod on rGO films	H_3PO_4-PVA	Micro electrode	973, 2.5 A g^{-1}	90%, 1700	[46]
PANI/carboxyl-rGO	1 M H_2SO_4	Three electrode	525, 0.3 A g^{-1}	91%, 200	[54]
PANI hollow spheres@rGO	1 M H_2SO_4	Three electrode	614, 1 A g^{-1}	90%, 500	[37]
PANI nanorod/rGO paper	1 M H_2SO_4	Three electrode	763, 1 A g^{-1}	82%, 1000	[91]
PANI-coupled Co_3O_4 and rGO	6 M KOH	Three electrode	1063, 1 A g^{-1}	95%, 2500	[88]
PANI on porous rGO film	1 M H_2SO_4	Two electrode	385, 0.5 A g^{-1}	88%, 5000	[61]
PANI/GO on stainless steel	1 M H_2SO_4	Two electrode	1136, 1 A g^{-1}	89%, 1000	[92]
PANI nanosphere/rGO film	0.5 M H_2SO_4	Three electrode	448, 1 A g^{-1}	81%, 5000	[36]
rGO/PANI gel on rGO paper	1 M H_2SO_4	Two electrode	864, 1 A g^{-1}	85%, 5000	[93]
PANI/rGO films	1 M H_2SO_4	Two electrode	431, 0.45 A g^{-1}	74%, 500	[22]
PANI nanowire on rGO foam	1 M H_2SO_4	Two electrode	790, 1 A g^{-1}	80%, 5000	[94]
PANI nanowire on rGO/ZrO_2	1 M H_2SO_4	Three electrode	1360, 1 A g^{-1}	93%, 1000	[95]
3D PANI on pillared rGO	0.5 M H_2SO_4	Two electrode	652, 1 A g^{-1}	90%, 4000	[48]
3D graphene/PANI nanorod	1 M H_2SO_4	Three electrode	1341, 0.5 A g^{-1}	70%, 5000	[21]
PANI/rGO woven-fabric films	H_3PO_4-PVA	Two electrode	23 mF cm^{-2}, 0.1 mA cm^{-2}	100%, 2000	[47]
3D graphene/PANI nanocone	1 M $HClO_4$	Three electrode	751.3, 1 A g^{-1}	93%, 1000	[96]
PANI/B-doped rGO	1 M H_2SO_4	Three electrode	406	90%, 10000	[79]
rGO hydrogel films embedded with PANI nanofibers	1 M H_2SO_4	Three electrode	921, 1 A g^{-1}	100%, 2000	[41]
PANI nanofibers/N-doped rGO hydrogels	1 M H_2SO_4	Three electrode	610, 1 A g^{-1}	94%, 1000	[67]
PANI nanofiber/rGO foam	1 M H_2SO_4	Three electrode	968, 0.31 A g^{-1}	83%, 15000	[97]
Phase-separated PANI/rGO	1 M H_2SO_4	Three electrode	783, 27.3 A g^{-1}	81%, 10000	[63]
PANI nanorods on rGO sponges	1 M H_2SO_4	Three electrode	662, 1 A g^{-1}	93%, 5000	[55]
PANI/rGO composite film	1 M H_2SO_4	Three electrode	1182, 1 A g^{-1}	108%, 10000	[42]
PANI/rGO composites	1 M H_2SO_4	Three electrode	524, 0.5 A g^{-1}	81%, 2000	[98]
PANI/rGO composite film	1 M H_2SO_4	Two electrode	763, 0.34 A g^{-1}	76%, 2000	[68]
PANI nanowire on rGO foam	1 M H_2SO_4	Two electrode	939, 1 A g^{-1}	88%, 5000	[99]

rGO sheets could achieve high capacitance of 569 F g^{-1} [40]. Fan et al. reported the fabrication of PANI hollow spheres@rGO composites with a capacitance of 614 F g^{-1} in 1.0 M H_2SO_4 at 1 A g^{-1}, where PANI hollow spheres showed enhanced surface-to-volume ratios and reduced transport lengths for both mass and charge transport [37].

2.2. In-situ polymerization methods

In-situ polymerization methods for the preparation of PANI/graphene nanocomposites can be mainly divided into two classes based on different reaction mechanisms: chemical oxidative methods and electrochemical oxidative methods. Chemical oxidative methods for the synthesis of PANI usually involved the use of oxidants such as ferric chlorides and ammonium persulfates [8,32]. Chemical oxidative synthesis provided conveniences for controlling the nucleation and growth process during in-situ polymerization of aniline on graphene. However, electrochemical oxidative procedures involved potentiostatic or galvanostatic deposition of aniline from electrolyte on the surface of graphene paper, 3D graphene and deposited graphene on substrates such as indium tin oxide (ITO) or polydimethylsiloxane (PDMS) [13,45–47]. Electrochemical oxidative polymerization could directly immobilize PANI on the graphene electrodes, which showed advantages for fabricating binder-free electrodes and maintaining PANI layer with a uniform thickness.

Though the in-situ oxidative polymerization procedures are straightforward and efficient, which can be easily scaled up for the commercial productions of PANI/graphene nanocomposites, it is a great challenge to achieve a uniform dispersion and chemical reactivity of graphene in the reaction mixture. In addition, the unavoidable re-stacking of graphene would result in considerably low surface area, which significantly hindered the polymerization of aniline along its surface and lead to the grains of bulk-phase PANI [48]. Given that, heavily oxygenated GO sheets were sometimes chosen as the starting materials for the growth of PANI [49]. Most PANI/graphene nanocomposites only utilized carboxyl edges of rGO to bond aniline, and the resultant rGO sheets were freely dangled by the edges from the PANI rather than being fixed by the basal planes [28,50–53].

In these cases, one of the effective strategies adopted to enhance the electrochemical performance of the PANI/graphene nanocomposites is by grafting organic molecules on graphene through covalent functionalization to form robust chemical combinations of graphene with aniline monomer as well as PANI [32,54–56]. Steric hindrances between the anchored molecules made graphene staying apart, which improved the ionic accessibility of graphene. The grafting procedure could also modify the basal planes of graphene with various oxygen-containing groups to provide additional active sites for sequent growth of PANI. Sulfonic acid groups functionalized graphene sheets as both substrates and acid dopants were prepared, and the resultant sulfonated graphene/PANI nanocomposites with imbedded PANI nanorods showed a high capacitance of 763 F g^{-1} with a good rate performance. The amount of the acid dopants played a significant role in tuning the morphology of the resultant nanocomposites, especially in controlling the morphologies of PANI on graphene [32]. Liu et al. developed naturally existing oxygenated groups into carboxyl groups on GO basal planes via a ring-opening reaction and an esterification reaction, which provided highly consistent affinity to polymerized PANI chains, and thus facilitated the formation of ordered PANI/graphene nanocomposites [54]. Benzoic acid anchored graphene was used as a support, and 3D PANI structures were achieved by a simple chemical oxidation of aniline in the presence of phytic acid (PA) [48]. The benzoic acid anchored graphene/PANI nanocomposites achieved a high conductivity of 3.74 S cm^{-1} and high surface area of 330 m^2 g^{-1}, which resulted in high specific capacitance of 652 F g^{-1}.

3. Electrode performances of PANI/graphene nanocomposites

The electrode performances of the PANI/graphene nanocomposites for supercapacitors are summarized in terms of electrolyte, cell configuration, specific capacitance and cycle life, as listed in Table 1. Several factors, including the morphologies, the synthesis/fabrication techniques, the component ratios of PANI and graphene, the doping level of PANI and the synthesis conditions by varying the sequence of compositing or reducing GO, adding a third component, changing the electrolytes, would definitely influence the electrochemical properties of PANI/graphene nanocomposites as electrode materials. These factors will be separately discussed in the following sections.

3.1. Morphologies of PANI/graphene nanocomposites

The design and synthesis of nanostructured PANI/graphene nanocomposites lead to high specific capacitances because they synergistically combined three key factors including high-capacitance active materials, high electrical conductivity for fast charge transfer, and unique porous structure for fast ion diffusions [57]. Basically, binders are required for fabricating powder-based PANI/graphene nanocomposites into electrodes, which inevitably affect the electrical conductivity and the overall electrochemical performances are compromised [8,28,58]. Given that, PANI/graphene composite films can be easily made and cut into binder-free electrodes, which can be fabricated by chemical or electrochemical oxidative polymerization of aniline on rGO paper or foam [59–61]. Besides, 3D porous PANI/graphene composite hydrogels as a binder-free electrode could be developed from the suspension of PANI nanofiber and GO through a hydrothermal process [62]. Generally, among such structures a free-standing graphene skeleton is required to achieve a high capacitance of PANI/graphene nanocomposites due to interconnected conductive network. However, most of the reported PANI/graphene nanocomposites with such structures cannot guarantee high rate performances because of the lack of efficient ion diffusions, which was not taken into accounts in these cases [8,30,59].

In order to obtain high rate performances for PANI/graphene nanocomposites, the microstructures of the nanocomposites should be optimized. 3D and flexible rGO films using $CaCO_3$ particles as sacrificial templates facilitated a porous structure within the 3D rGO, and then PANI nanowire arrays were grown on 3D rGO by chemical oxidative polymerizations [61]. The specific capacitance of the 3D rGO/PANI film maintained at 88% when the current density increased from 0.5 to 10 A g^{-1}. The formation of PANI nanowire arrays was a key factor in maintaining high rate performances because almost every PANI nanowire could access the electrolytic ions and participate in the electrochemical reactions, as exhibited in Fig. 2. Another example was the growth of PANI onto a graphene monolith with a phase-separated structure [63]. The phase-separated PANI/graphene nanostructures were beneficial to an efficient diffusion of electrolytic ions as well as large capacitive enhancements of PANI/graphene nanocomposites at a large current density, compared with uniformly structured PANI/graphene nanocomposites. A high capacitance of 783 F g^{-1} was achieved at a high current density of 27.3 A g^{-1}. A possible mechanism to explain the poor performance of uniformly structured PANI/graphene nanocomposites was proposed that large lateral sizes and aspect ratios of graphene might act as inevitable barriers to the ion diffusions. Given that, Zhang et al. immobilized PANI nanoparticles onto a conductive film substrate utilizing graphene and CNTs as building blocks, thus to obtain flexible PANI/graphene/CNT ternary composite films with a hierarchical nanostructure. The ternary PANI/graphene/CNT nanocomposite film exhibited a specific capacitance up to 432 F g^{-1} at 0.5 A g^{-1}, and dramatically enhanced cycling stability. The dimensional confinement of PANI particles on the surface of the conductive graphene/CNT composite films prohibited large volume expansion/shrinkage upon cycling, and meanwhile, the immobilized PANI particles endowed the nanocomposite films with additional pseudocapacitive behaviors and improved interfaces between electrode and electrolyte [64]. In addition, Fan et al. prepared a ternary PANI/graphene/CNT composite film by polymerizing PANI onto a 3D porous graphene/CNT composite film substrate, exhibiting a high capacitance of 409 F g^{-1} at 10 A g^{-1}, as well as excellent rate and cycling performances [65].

3.2. Synthesis/fabrication techniques of PANI/graphene nanocomposites

Compositing PANI with rGO has been widely investigated and the capacitive enhancements greatly depend on different synthesis/fabrication techniques [27,30,58,64,66]. In other words, the synthesis/fabrication techniques have large influences on the electrochemical performances mainly depending on the different combinations between the two components.

Tailoring nanostructured PANI on rGO and grafting PANI on graphene are efficient strategies for the construction of PANI/graphene nanocomposites. A novel strategy was proposed to prepare PANI and PANI/graphene hydrogels: (1) 3D dendritic PANI nanofiber hydrogels, (2) dendritic PANI nanofiber/graphene hydrogels and (3) PANI nanofiber/N-doped graphene hydrogels [67]. This strategy involved an integrated route of polymerization of aniline followed by a hydrothermal process. Although high capacitances could be achieved for constructing 3D graphene/PANI nanocomposites, these 3D porous nanocomposites were usually prepared in rather complicated processes, such as using sacrificial templates and hydrothermal methods, which unavoidably hindered scale-up productions of such composite structures.

A key difficulty in constructing 3D rGO structures is how to prevent rGO sheets from restacking without introducing sacrificial templates, and meanwhile avoid high-cost synthetic procedures. To solve the issue, Yu et al. presented a template-free and cost-effective approach for large-scale fabrication of high-quality 3D graphene-based frameworks (3DGFs) from commercial graphite paper at mild conditions [21]. The synthetic procedures, photographs and SEM images of macroscopically porous 3DGFs are illustrated in Fig. 3. The volume expansion happened during the graphite exfoliating process by modified Hummer's method, which was quite possible to realize large scale synthesis of 3DGFs by just enlarging the equipment. When used as a 3D substrate to load PANI, the PANI nanorods exhibited a high specific capacitance of 1341.3 F g^{-1} (596.1 F g^{-1} based on the mass of the whole electrode) at 0.5 A g^{-1}. In addition, Hong et al. fabricated a binder-free rGO/PANI electrode utilizing diffusion driven layer-by-layer (dd-LbL) assembly based on electrostatic interactions between GO and branched polyethyleneimine (PEI) to build a 3D foam-like GO structure, which exhibited a high specific capacitance of 438.8 F g^{-1} at 0.5 A g^{-1} [68].

3.3. Component ratios of PANI and graphene

In most cases, the low-density PANI/grapheme nanocomposites might result in low volumetric capacitances of the nanocomposites. It is a challenge to enlarge volumetric capacitances of the nanocomposites by a compact assembly of individual components while maintaining their high gravimetric capacitances. The self-assembly methods enabled the tunable compositions of the PANI/graphene nanocomposites with tailorable PANI contents over a wide range. Hu et al. fabricated 3D skeleton networks of graphene-wrapped PANI nanofibers with four different PANI contents (5 wt%,10 wt%, 50 wt% and 80 wt%), and the hydrogel films with the PANI contents lower than 50 wt% were robust for flexible supercapacitors [42]. With the increase of PANI contents from 0% to 100%, the gravimetric capacitances of the resultant electrodes first increased and then decreased. A high specific capacitance value of 921 F g^{-1} at 1 A g^{-1} can be obtained by rGO-PANI (50 wt%) hydrogel film, which was much higher than that of rGO hydrogel film (128 F g^{-1}) and PANI nanofibers (575 F g^{-1}). The contents of PANI within the PANI/graphene nanocomposites prepared by in-situ polymerization methods also influenced the electrochemical performances

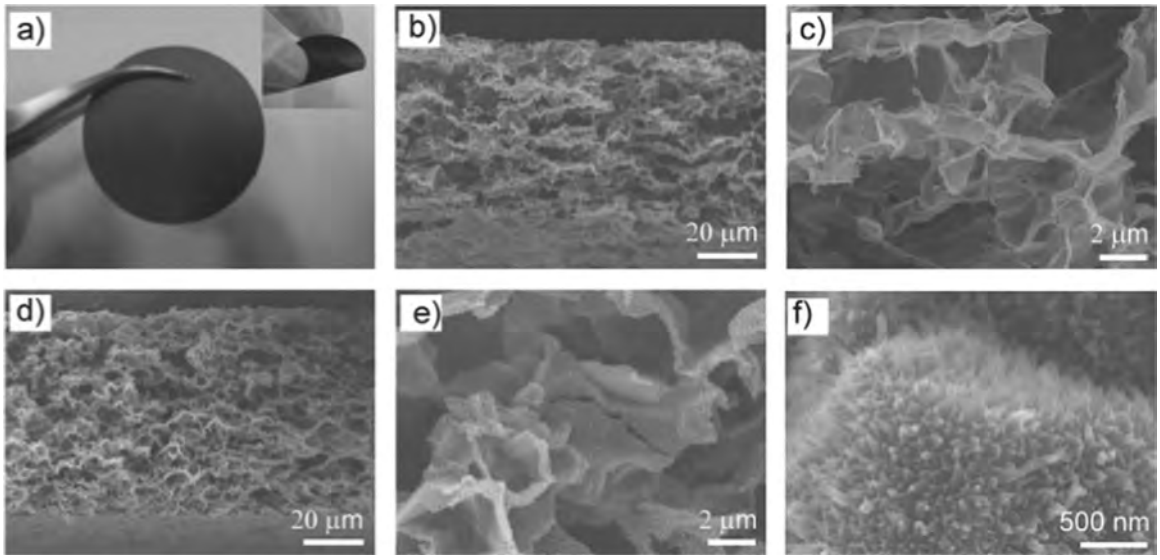

Fig. 2. Morphologies of 3D-rGO and 3D-rGO/PANI films. (a) Digital images, with the inserted image showing the flexibility of the film. Cross-section SEM images of (b, c) 3D-rGO and (D-f) 3D-rGO/PANI films at different magnifications [61]. Reprinted with permission from Ref. [61], Copyright 2013, Wiley-VCH.

of the nanocomposites. Xu et al. reported a PANI/graphene composite monolith as a self-standing electrode with a density over 1.5 g cm^{-3}, which exhibited a record high volumetric capacitance over 800 F cm^{-3} [69]. In particular, the growing process of PANI in PANI/graphene composite monoliths was monitored by SEM observations, as shown in Fig. 4. A similar tendency of the capacitive performances revealed that the specific capacitance increased with the PANI loadings up to 54%, but higher PANI loadings did not bring in additional capacitances. Moreover, the nanocomposites with the PANI content higher than 54% show larger ion diffusion resistance and fast decay of the capacitance at a large current density.

3.4. PANI doping level in PANI/graphene nanocomposites

Doping the PANI chains with an oxidizing component (p-type) or reducing component (n-type) alters the charge distribution over the π orbitals, which is a key requirement for achieving high-performance electrochemical performances of PANI [12]. Hence, the doping, whether during or after polymerization, is highly responsible for resultant electrochemical behaviors. Hu et al. employed an Ir-doped PANI film electrode with an operating voltage window up to 0.7 ~ 0.8 V. The specific capacitances of PANI strongly depended on the doping level. Noted that the initial doping is not an essential process to make PANI an active material [70,71]. Bian et al. showed that the specific capacitance of a de-doped PANI is 29% higher than that of doped PANI [72]. The reason was that some dopants covalently attached to PANI chains blocked parts of the capacitances. De-doping also resulted in morphological changes promoting the formation of micropores, which would achieve a better accessibility of active materials with ions. Nevertheless, initial doping was typically used as an internal template for controlling the shape of PANI network, which was directly responsible for the electrochemical performances [73–75].

Wang et al. presented a three-step synthesis method for the preparation of PANI/graphene nanocomposites by in-situ polymerization/

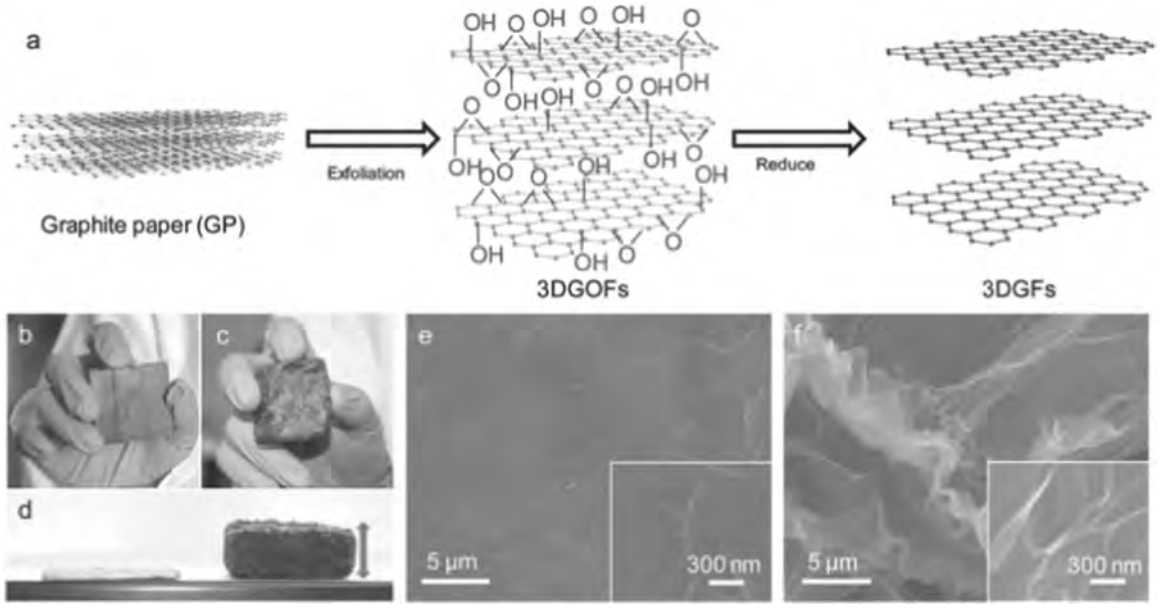

Fig. 3. (a) Schematic diagram illustrating the fabrication of 3DGFs. Photographs of (b) GP, (c) 3DGFs, and (d) their comparison. SEM images of (e) GP and (f) 3DGFs [21]. Reprinted with permission from Ref. [21], Copyright 2015, Wiley-VCH.

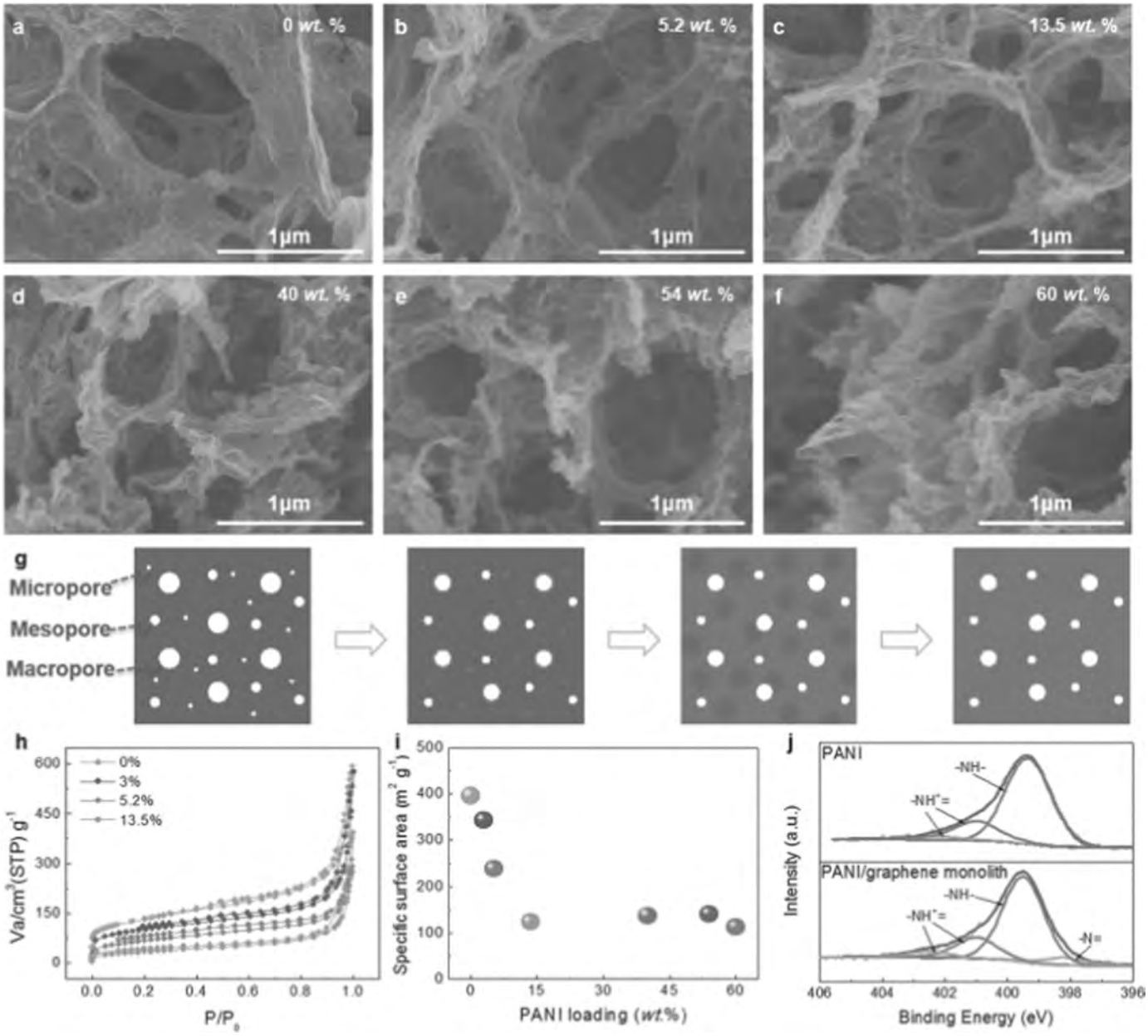

Fig. 4. Growing process of PANI in PANI/graphene composite monoliths. (a-f) SEM images of freeze-dried PANI/graphene nanocomposites with PANI loadings from 0% to 60%. (g) 2D schematic representation of growing process of PANI in 3D grapheme monoliths with the increase of PANI loadings from a transmission view. (h) Nitrogen adsorption/desorption isotherms and (i) specific surface area of freeze-dried PANI/graphene nanocomposites with different PANI loadings showing that aniline is preferentially grown around the micropores and blocks [69]. Reprinted with permission from Ref. [69], Copyright 2015, Wiley-VCH.

reduction/dedoping-redoping process [8]. Although the redoping process lead to little decreases of capacitances from 1126 F g^{-1} to 1079 F g^{-1}, energy densities of the electrodes of 37.9 Wh kg^{-1} at the power densities of 141.1 W kg^{-1} were better than the nanocomposites after reduction/dedoping. Hao et al. noticed that the introduction of additional acids and the ratios of sulfonated graphene to aniline played a significant role in controlling the morphology of the nanocomposites [32]. The low concentration of protons from sulfonated graphene acting as macromolecular dopants restrained the growth speed of PANI nuclei on sulfonated grapheme and promoted the formation of high-crystalline PANI nanorods. As a result, the nanocomposites exhibited specific capacitance values of 763 F g^{-1} with better rate performances than both sulfonated graphene and additional HCl doped nanocomposites.

3.5. Synthesis conditions for PANI/graphene nanocomposites

There are several synthesis conditions by varying the sequence of compositing or reducing GO, adding a third component, changing the electrolytes, which would greatly influence the capacitive properties of the PANI/graphene nanocomposites. In most cases, rGO was first achieved from GO and then followed by compositing with PANI, which might greatly affect the disperse states of graphene and the electrochemical properties of the nanocomposites [76–78]. A PANI/graphene nanocomposite was made by reducing GO using hydrazine hydrate in presence of PANI [28]. However, the specific capacitances can be only 480 F g^{-1}. Although this kind of strategy benefited to form a homogeneous dispersion of PANI and GO, the follow-up reduction procedures from GO to rGO might dedope the PANI with a decay of capacitive performances. Feng et al. noticed that GO precursors could be electrochemically reduced to graphene at cathodic potentials, and

meanwhile, aniline monomer can be polymerized at anodic potentials. Based on these two points, they developed a new one-step electrochemical synthesis of PANI/graphene composite film in a large scale by scanning the potential of the electrode between -1.3 and 1.0 V by using GO and aniline as the starting materials, achieving a specific capacitance value of 640 F g^{-1} [45]. Hao et al. designed a novel PANI/graphene nanocomposite where boron-doped graphene were used as substrates for loading PANI by in-situ polymerization [79]. More specifically, they investigated the capacitive performances of the nanocomposites in both acid and alkaline electrolytes. The electrochemical impedance spectroscopy (EIS) plots before and after cycling tests in 1 M H_2SO_4 illustrated only slight changes at high and low frequency regions. However, compared with the plot before cycling in alkaline electrolyte, the charge-transfer resistance was about 8 Ω and the slop at low frequency greatly changed, nearly to a half of original value after 5000 cycles. This result was probably related to the electrochemical actives of PANI in different electrolytes. The conductivity of PANI would decrease because of the de-protonation for long-time immersions. Brozova et al. reported that the mass of PANI was constantly lost by removals of residual adsorbed water or aniline oligomers, when PANI was immersed in alkaline [80].

Adding a third component such as metal nanoparticles or metal oxides/hydroxides into the PANI/graphene nanocomposites is a manageable approach to optimize the capacitive performances of the nanocomposites [81–84]. The strong coupling between metal oxide/hydroxide nanoparticles and graphene in a confined 2D manner gave the nanocomposites with unique structural features and synergistic electrochemical properties derived from individual components [85–87]. For instances, Li et al. demonstrated an efficient and universal strategy for controlled growth of metal oxides/hydroxides (such as Co_3O_4, Fe_2O_3, and $Ni(OH)_2$) nanoparticles on graphene to construct unique 2D graphene hybrids employing PANI as coupling linkers between the two components [88]. Remarkably, the specific capacitance of the PANI/graphene/Co_3O_4 electrode could be maintained at 1010 F g^{-1} (> 95% capacitance retention) after 2500 cycles.

4. Summary and outlook

In summary, we presented a state-of-the-art review of recent advances in the design, synthesis and applications of the PANI/graphene nanocomposites as electrode materials for supercapacitors. Upon rational design and synthesis, the PANI/graphene nanocomposites have achieved high specific capacitance, high powder density and remarkable cycling stability. However, the vastly different performance of various PANI/graphene nanocomposites in literatures pushed us to investigate the differences and key factors determining the electrochemical performances of the nanocomposites, such as the morphologies, synthesis/fabrication methods and synthesis conditions. The optimized synthesis conditions and prerequisites for improving the electrochemical capacitive performances of PANI/graphene nanocomposites were discussed in details. Several basic necessities for measuring and analyzing the capacitive performances of PANI/graphene nanocomposites were also reviewed.

Future research directions of the development of PANI/graphene nanocomposites are proposed. First, the PANI/graphene nanocomposites are mostly arbitrated on the specific capacitances and cycling abilities, while there are other characteristics that should be noted to provide a complete assessment system. For instance, the energy density, i.e. the storage capacity, and the power density, i.e. the speed of charge/discharge, are not always revealed in a scientific paper, which might lead to a false conclusion regarding the status and potentials of the PANI/graphene composite electrodes for supercapacitors. In addition, the cycling stability should be analyzed and reported for a large number of cycles (> 10000) considering the practical applications of supercapacitors. Hence, the researchers should be encouraged to provide a comprehensive analysis of the electrochemical performances of the PANI/graphene nanocomposites.

On practical and research forefronts, there is a need to improve the existing routes and develop new preparation methods for fabrication of PANI/graphene nanocomposites. Two major goals towards the fabrication of PANI/graphene nanocomposites are the scale-up production of PANI/graphene nanocomposites and the introduction of hierarchical porous structures within PANI/graphene nanocomposites. One possible strategy achieving the scale-up production of PANI/graphene nanocomposites is to utilize naturally existing materials as the starting materials. Besides, inspired by the phase-separated PANI/graphene nanocomposites that the intrinsic large lateral size and aspect ratio of grapheme might hinder the electrolyte diffusions [63]. Therefore, inducing defects on the graphene planes could be taken into considerations to construct hierarchical porous electrodes.

There are a number of advantages associated with appropriate functionalizations of graphene towards the PANI/graphene nanocomposites, which not only improves the interface interactions between PANI and graphene, but also allows boosting the capacitive performances with high contents of graphene within PANI/graphene nanocomposites. With higher contents of graphene, improved ionic accessibility through electrolyte channels and better capacitive properties of the resultant nanocomposites can be achieved. Moreover, the formation of ternary nanocomposites by introducing CNTs or metal oxides into the PANI/grapheme nanocomposites may yield additional capacitive performance benefits. However, it is still a challenge to improve the interfacial interactions in binary or ternary PANI/graphene nanocomposites.

On theoretical forefront, it is urgent to investigate and explain the charging mechanism of PANI/graphene nanocomposites for supercapacitors. Several researchers have tried to probe the charging mechanism of PANI or graphene alone in various electrolytes, but the exact charging mechanism of PANI/graphene nanocomposites is still not fully known. Recently, Xu et al. proposed a proton transport mechanism of PANI in dense nanocomposites, indicating that PANI was a dual electronic-ionic conductivity polymer that acted not only as a pseudocapacitive active material for high energy storage but also as a proton conductor that realized a proton transport from the interfaces of electrode/electrolyte to the inner of dense particles [89]. More importantly, they further proposed the design principle of non-porous carbon nanocomposites to achieve high volumetric performances, in which a good dual electronic-ionic conductor was selected as optimized pseudocapacitive additives. Therefore, it is essential to identify the charging mechanism in order to fully understand and exploit the capacitive properties of PANI/graphene nanocomposites. In retrospect, we can safely say that the PANI/graphene nanocomposites have an ability to make high-performance supercapacitors, but more should be done to meet the future requirements of next-generation supercapacitors.

Acknowledgements

This work was supported by the National Natural Science Foundation of China (51433001, 21504012 and 51773035), the Fundamental Research Funds for the Central Universities (17D110606), the Program of Shanghai Subject Chief Scientist (17XD1400100) and the Natural Science Foundation of Shanghai (17ZR1439900).

References

[1] R. Kötz, M. Carlen, Principles and applications of electrochemical capacitors, Electrochim. Acta 45 (2000) 2483–2498.
[2] J.R. Miller, P. Simon, Electrochemical capacitors for energy management, Science 321 (2008) 651–652.
[3] P. Simon, Y. Gogotsi, Materials for electrochemical capacitors, Nat. Mater. 7 (2008) 845–854.
[4] M.D. Stoller, S. Park, Y. Zhu, J. An, R.S. Ruoff, Graphene-based ultracapacitors, Nano Lett. 8 (2008) 3498–3502.

[5] Y. Gogotsi, P. Simon, True performance metrics in electrochemical energy storage, Science 334 (2011) 917–918.
[6] X. Yang, C. Cheng, Y. Wang, L. Qiu, D. Li, Liquid-mediated dense integration of graphene materials for compact capacitive energy storage, Science 341 (2013) 534–537.
[7] D. Li, J. Huang, R.B. Kaner, Polyaniline nanofibers: a unique polymer nanostructure for versatile applications, Acc. Chem. Res. 42 (2008) 135–145.
[8] H. Wang, Q. Hao, X. Yang, L. Lu, X. Wang, A nanostructured graphene/polyaniline hybrid material for supercapacitors, Nanoscale 2 (2010) 2164–2170.
[9] P.J. Bora, K.J. Vinoy, P.C. Ramamurthy, Kishore, G. Madras, Electromagnetic interference shielding effectiveness of polyaniline-nickel oxide coated cenosphere composite film, Comp. Comm. 4 (2017) 37–42.
[10] H. Li, J. Wang, Q. Chu, Z. Wang, F. Zhang, S. Wang, Theoretical and experimental specific capacitance of polyaniline in sulfuric acid, J. Power Sources 190 (2009) 578–586.
[11] W.-S. Huang, B.D. Humphrey, A.G. MacDiarmid, Polyaniline, a novel conducting polymer. Morphology and chemistry of its oxidation and reduction in aqueous electrolytes, J. Chem. Soc., Faraday Trans. 82 (1986) 2385–2400.
[12] A. Eftekhari, L. Li, Y. Yang, Polyaniline supercapacitors, J. Power Sources 347 (2017) 86–107.
[13] D.-W. Wang, F. Li, J. Zhao, W. Ren, Z.-G. Chen, J. Tan, Z.-S. Wu, I. Gentle, G.Q. Lu, H.-M. Cheng, Fabrication of graphene/polyaniline composite paper via in situ anodic electropolymerization for high-performance flexible electrode, ACS Nano 3 (2009) 1745–1752.
[14] Q. Wu, Y. Xu, Z. Yao, A. Liu, G. Shi, Supercapacitors based on flexible graphene/polyaniline nanofiber composite films, ACS Nano 4 (2010) 1963–1970.
[15] T.J. Booth, P. Blake, R.R. Nair, D. Jiang, E.W. Hill, U. Bangert, A. Bleloch, M. Gass, K.S. Novoselov, M.I. Katsnelson, Macroscopic graphene membranes and their extraordinary stiffness, Nano Lett. 8 (2008) 2442–2446.
[16] C. Lee, X. Wei, J.W. Kysar, J. Hone, Measurement of the elastic properties and intrinsic strength of monolayer graphene, science 321 (2008) 385–388.
[17] J. Xia, F. Chen, J. Li, N. Tao, Measurement of the quantum capacitance of graphene, Nat. Nanotechnol. 4 (2009) 505–509.
[18] H. Li, L. Xu, H. Sitinamaluwa, K. Wasalathilake, C. Yan, Coating Fe2O3 with graphene oxide for high-performance sodium-ion battery anode, Comp. Comm. 1 (2016) 48–53.
[19] T. Wang, J. Yu, M. Wang, Y. Cao, W. Dai, D. Shen, L. Guo, Y. Wu, H. Bai, D. Dai, J. Lyu, N. Jiang, C. Pan, C.-T. Lin, Effect of different sizes of graphene on thermal transport performance of graphene paper, Comp. Comm. 5 (2017) 46–53.
[20] Q. Wu, Y. Sun, H. Bai, G. Shi, High-performance supercapacitor electrodes based on graphene hydrogels modified with 2-aminoanthraquinone moieties, Phys. Chem. Chem. Phys. 13 (2011) 11193–11198.
[21] M. Yu, Y. Huang, C. Li, Y. Zeng, W. Wang, Y. Li, P. Fang, X. Lu, Y. Tong, Building three-dimensional graphene frameworks for energy storage and catalysis, Adv. Funct. Mater. 25 (2015) 324–330.
[22] M. Kim, C. Lee, J. Jang, Fabrication of highly flexible, scalable, and high-performance supercapacitors using polyaniline/reduced graphene oxide film with enhanced electrical conductivity and crystallinity, Adv. Funct. Mater. 24 (2014) 2489–2499.
[23] N.A. Kumar, H.-J. Choi, Y.R. Shin, D.W. Chang, L. Dai, J.-B. Baek, Polyaniline-grafted reduced graphene oxide for efficient electrochemical supercapacitors, ACS Nano 6 (2012) 1715–1723.
[24] Ce.NeR. Rao, Ae.K. Sood, Ke.S. Subrahmanyam, A. Govindaraj, Graphene: the new two-dimensional nanomaterial, Angew. Chem. Int. Ed. 48 (2009) 7752–7777.
[25] H. Bai, Y. Xu, L. Zhao, C. Li, G. Shi, Non-covalent functionalization of graphene sheets by sulfonated polyaniline, Chem. Commun. (2009) 1667–1669.
[26] T. Lee, T. Yun, B. Park, B. Sharma, H.-K. Song, B.-S. Kim, Hybrid multilayer thin film supercapacitor of graphene nanosheets with polyaniline: importance of establishing intimate electronic contact through nanoscale blending, J. Mater. Chem. 22 (2012) 21092–21099.
[27] J. Xu, K. Wang, S.-Z. Zu, B.-H. Han, Z. Wei, Hierarchical nanocomposites of polyaniline nanowire arrays on graphene oxide sheets with synergistic effect for energy storage, ACS Nano 4 (2010) 5019–5026.
[28] K. Zhang, L.L. Zhang, X.S. Zhao, J. Wu, Graphene/polyaniline nanofiber composites as supercapacitor electrodes, Chem. Mater. 22 (2010) 1392–1401.
[29] L.Q. Xu, Y.L. Liu, K.-G. Neoh, E.-T. Kang, G.D. Fu, Reduction of graphene oxide by aniline with its concomitant oxidative polymerization, Macromol. Rapid Commun. 32 (2011) 684–688.
[30] X.M. Feng, R.M. Li, Y.W. Ma, R.F. Chen, N.E. Shi, Q.L. Fan, W. Huang, One-step electrochemical synthesis of graphene/polyaniline composite film and its applications, Adv. Funct. Mater. 21 (2011) 2989–2996.
[31] M. Xue, F. Li, J. Zhu, H. Song, M. Zhang, T. Cao, Structure-based enhanced capacitance: in situ growth of highly ordered polyaniline nanorods on reduced graphene oxide patterns, Adv. Funct. Mater. 22 (2012) 1284–1290.
[32] Q. Hao, H. Wang, X. Yang, L. Lu, X. Wang, Morphology-controlled fabrication of sulfonated graphene/polyaniline nanocomposites by liquid/liquid interfacial polymerization and investigation of their electrochemical properties, Nano Res. 4 (2011) 323–333.
[33] H.Y. He, J. Klinowski, M. Forster, A. Lerf, A new structural model for graphite oxide, Chem. Phys. Lett. 287 (1998) 53–56.
[34] A. Lerf, H. He, M. Forster, J. Klinowski, Structure of graphite oxide revisited‖, J. Phys. Chem. B 102 (1998) 4477–4482.
[35] J. Huang, R.B. Kaner, A general chemical route to polyaniline nanofibers, J. Am. Chem. Soc. 126 (2004) 851–855.
[36] M. Hassan, K.R. Reddy, E. Haque, S.N. Faisal, S. Ghasemi, A.I. Minett, V.G. Gomes, Hierarchical assembly of graphene/polyaniline nanostructures to synthesize free-standing supercapacitor electrode, Compos. Sci. Technol. 98 (2014) 1–8.
[37] W. Fan, C. Zhang, W.W. Tjiu, K.P. Pramoda, C. He, T. Liu, Graphene-wrapped polyaniline hollow spheres as novel hybrid electrode materials for supercapacitor applications, ACS Appl. Mater. Interfaces 5 (2013) 3382–3391.
[38] D. Li, R.B. Kaner, Processable stabilizer-free polyaniline nanofiber aqueous colloids, Chem. Commun. (2005) 3286–3288.
[39] D. Li, M.B. Müller, S. Gilje, R.B. Kaner, G.G. Wallace, Processable aqueous dispersions of graphene nanosheets, Nat. Nanotechnol. 3 (2008) 101–105.
[40] X. Lu, H. Dou, S. Yang, L. Hao, L. Zhang, L. Shen, F. Zhang, X. Zhang, Fabrication and electrochemical capacitance of hierarchical graphene/polyaniline/carbon nanotube ternary composite film, Electrochim. Acta 56 (2011) 9224–9232.
[41] N. Hu, L. Zhang, C. Yang, J. Zhao, Z. Yang, H. Wei, H. Liao, Z. Feng, A. Fisher, Y. Zhang, Z.J. Xu, Three-dimensional skeleton networks of graphene wrapped polyaniline nanofibers: an excellent structure for high-performance flexible solid-state supercapacitors, Sci. Rep. 6 (2016).
[42] L. Zhang, D. Huang, N. Hu, C. Yang, M. Li, H. Wei, Z. Yang, Y. Su, Y. Zhang, Three-dimensional structures of graphene/polyaniline hybrid films constructed by steamed water for high-performance supercapacitors, J. Power Sources 342 (2017) 1–8.
[43] D. Yu, L. Dai, Self-assembled graphene/carbon nanotube hybrid films for supercapacitors, J. Phys. Chem. Lett. 1 (2009) 467–470.
[44] X. Lu, H. Dou, B. Gao, C. Yuan, S. Yang, L. Hao, L. Shen, X. Zhang, A flexible graphene/multiwalled carbon nanotube film as a high performance electrode material for supercapacitors, Electrochim. Acta 56 (2011) 5115–5121.
[45] X.-M. Feng, R.-M. Li, Y.-W. Ma, R.-F. Chen, N.-E. Shi, Q.-L. Fan, W. Huang, One-step electrochemical synthesis of graphene/polyaniline composite film and its applications, Adv. Funct. Mater. 21 (2011) 2989–2996.
[46] M. Xue, F. Li, J. Zhu, H. Song, M. Zhang, T. Cao, Structure-based enhanced capacitance: in situ growth of highly ordered polyaniline nanorods on reduced graphene oxide patterns, Adv. Funct. Mater. 22 (2012) 1284–1290.
[47] X. Zang, X. Li, M. Zhu, X. Li, Z. Zhen, Y. He, K. Wang, J. Wei, F. Kang, H. Zhu, Graphene/polyaniline woven fabric composite films as flexible supercapacitor electrodes, Nanoscale 7 (2015) 7318–7322.
[48] P. Sekar, B. Anothumakkool, S. Kurungot, 3D polyaniline porous layer anchored pillared graphene sheets: enhanced interface joined with high conductivity for better charge storage applications, ACS Appl. Mater. Interfaces 7 (2015) 7661–7669.
[49] S. Park, R.S. Ruoff, Chemical methods for the production of graphenes, Nat. Nanotechnol. 4 (2009) 217–224.
[50] K.-S. Kim, I.-Y. Jeon, S.-N. Ahn, Y.-D. Kwon, J.-B. Baek, Edge-functionalized graphene-like platelets as a co-curing agent and a nanoscale additive to epoxy resin, J. Mater. Chem. 21 (2011) 7337–7342.
[51] C. Basavaraja, W.J. Kim, Y. Do Kim, Synthesis of polyaniline-gold/graphene oxide composite and microwave absorption characteristics of the composite films, Mater. Lett. 65 (2011) 3120–3123.
[52] L. Mao, K. Zhang, H.S.O. Chan, J. Wu, Surfactant-stabilized graphene/polyaniline nanofiber composites for high performance supercapacitor electrode, J. Mater. Chem. 22 (2012) 80–85.
[53] M. Liu, Y.E. Miao, C. Zhang, W.W. Tjiu, Z. Yang, H. Peng, T.X. Liu, Hierarchical composites of polyaniline-graphene nanoribbons-carbon nanotubes as electrode materials in all-solid-state supercapacitors, Nanoscale 5 (2013) 7312–7320.
[54] Y. Liu, R. Deng, Z. Wang, H. Liu, Carboxyl-functionalized graphene oxide-polyaniline composite as a promising supercapacitor material, J. Mater. Chem. 22 (2012) 13619–13624.
[55] K.H.S. Iessa, Y. Zhang, G. Zhang, F. Xiao, S. Wang, Conductive porous sponge-like ionic liquid-graphene assembly decorated with nanosized polyaniline as active electrode material for supercapacitor, J. Power Sources 302 (2016) 92–97.
[56] P. Huang, L. Jing, H. Zhu, X. Gao, Diazonium functionalized graphene: microstructure, electric, and magnetic properties, Acc. Chem. Res. 46 (2012) 43–52.
[57] Z. Ma, X. Zhao, C. Gong, J. Zhang, J. Zhang, X. Gu, L. Tong, J. Zhou, Z. Zhang, Preparation of a graphene-based composite aerogel and the effects of carbon nanotubes on preserving the porous structure of the aerogel and improving its capacitor performance, J. Mater. Chem. A 3 (2015) 13445–13452.
[58] Y. Liu, Y. Ma, S. Guang, H. Xu, X. Su, Facile fabrication of three-dimensional highly ordered structural polyaniline–graphene bulk hybrid materials for high performance supercapacitor electrodes, J. Mater. Chem. A 2 (2014) 813–823.
[59] Y. Wang, X. Yang, L. Qiu, D. Li, Revisiting the capacitance of polyaniline by using graphene hydrogel films as a substrate: the importance of nano-architecturing, Energy Environ. Sci. 6 (2013) 477–481.
[60] H.-P. Cong, X.-C. Ren, P. Wang, S.-H. Yu, Flexible graphene–polyaniline composite paper for high-performance supercapacitor, Energy Environ. Sci. 6 (2013) 1185–1191.
[61] Y. Meng, K. Wang, Y. Zhang, Z. Wei, Hierarchical porous graphene/polyaniline composite film with superior rate performance for flexible supercapacitors, Adv. Mater. 25 (2013) 6985–6990.
[62] Z. Niu, L. Liu, L. Zhang, Q. Shao, W. Zhou, X. Chen, S. Xie, A universal strategy to prepare functional porous graphene hybrid architectures, Adv. Mater. 26 (2014) 3681–3687.
[63] J. Wu, Qe Zhang, Aa Zhou, Z. Huang, H. Bai, L. Li, Phase-separated polyaniline/graphene composite electrodes for high-rate electrochemical supercapacitors, Adv. Mater. 28 (2016) 10211–10216.
[64] J. Zhu, W. Sun, D. Yang, Y. Zhang, H.H. Hoon, H. Zhang, Q. Yan, Multifunctional architectures constructing of PANI nanoneedle arrays on MoS2 thin nanosheets for high-energy supercapacitors, Small 11 (2015) 4123–4129.
[65] W. Fan, Y.-E. Miao, L. Zhang, Y. Huang, T.X. Liu, Porous graphene–carbon nanotube hybrid paper as a flexible nano-scaffold for polyaniline immobilization and

application in all-solid-state supercapacitors, RSC Adv. 5 (2015) 31064–31073.
[66] L. Li, A.-R.O. Raji, H. Fei, Y. Yang, E.L.G. Samuel, J.M. Tour, Nanocomposite of polyaniline nanorods grown on graphene nanoribbons for highly capacitive pseudocapacitors, ACS Appl. Mater. Interfaces 5 (2013) 6622–6627.
[67] J. Luo, W. Zhong, Y. Zou, C. Xiong, W. Yang, Preparation of morphology-controllable polyaniline and polyaniline/graphene hydrogels for high performance binder-free supercapacitor electrodes, J. Power Sources 319 (2016) 73–81.
[68] X. Hong, B. Zhang, E. Murphy, J. Zou, F. Kim, Three-dimensional reduced graphene oxide/polyaniline nanocomposite film prepared by diffusion driven layer-by-layer assembly for high-performance supercapacitors, J. Power Sources 343 (2017) 60–66.
[69] Y. Xu, Y. Tao, X. Zheng, H. Ma, J. Luo, F. Kang, Q.-H. Yang, A metal-free supercapacitor electrode material with a record high volumetric capacitance over 800 F cm(-3), Adv. Mater. 27 (2015) 8082–8087.
[70] C.-C. Hu, C.-H. Chu, Electrochemical and textural characterization of iridium-doped polyaniline films for electrochemical capacitors, Mater. Chem. Phys. 65 (2000) 329–338.
[71] C.-C. Hu, C.-H. Chu, Electrochemical impedance characterization of polyaniline-coated graphite electrodes for electrochemical capacitors—effects of film coverage/thickness and anions, J. Electroanal. Chem. 503 (2001) 105–116.
[72] C. Bian, A. Yu, De-doped polyaniline nanofibres with micropores for high-rate aqueous electrochemical capacitor, Synth. Met. 160 (2010) 1579–1583.
[73] W. Wu, D. Pan, Y. Li, G. Zhao, L. Jing, S. Chen, Facile fabrication of polyaniline nanotubes using the self-assembly behavior based on the hydrogen bonding: a mechanistic study and application in high-performance electrochemical supercapacitor electrode, Electrochim. Acta 152 (2015) 126–134.
[74] Y. Gawli, A. Banerjee, D. Dhakras, M. Deo, D. Bulani, P. Wadgaonkar, M. Shelke, S. Ogale, 3D polyaniline architecture by concurrent inorganic and organic acid doping for superior and robust high rate supercapacitor performance, Sci. Rep. 6 (2016) 21002.
[75] S. Giri, D. Ghosh, C.K. Das, In situ synthesis of cobalt doped polyaniline modified graphene composites for high performance supercapacitor electrode materials, J. Electroanal. Chem. 697 (2013) 32–45.
[76] G. Zhou, D.-W. Wang, F. Li, L. Zhang, N. Li, Z.-S. Wu, L. Wen, G.Q. Lu, H.-M. Cheng, Graphene-wrapped Fe3O4 anode material with improved reversible capacity and cyclic stability for lithium ion batteries, Chem. Mater. 22 (2010) 5306–5313.
[77] J. Yan, T. Wei, B. Shao, Z. Fan, W. Qian, M. Zhang, F. Wei, Preparation of a graphene nanosheet/polyaniline composite with high specific capacitance, Carbon 48 (2010) 487–493.
[78] A.V. Murugan, T. Muraliganth, A. Manthiram, Rapid, facile microwave-solvothermal synthesis of graphene nanosheets and their polyaniline nanocomposites for energy strorage, Chem. Mater. 21 (2009) 5004–5006.
[79] Q. Hao, X. Xia, W. Lei, W. Wang, J. Qiu, Facile synthesis of sandwich-like polyaniline/boron-doped graphene nano hybrid for supercapacitors, Carbon 81 (2015) 552–563.
[80] L. Brožová, P. Holler, J. Kovářová, J. Stejskal, M. Trchová, The stability of polyaniline in strongly alkaline or acidic aqueous media, Polym. Degrad. Stab. 93 (2008) 592–600.
[81] M. Sathish, S. Mitani, T. Tomai, I. Honma, MnO2 assisted oxidative polymerization of aniline on graphene sheets: superior nanocomposite electrodes for electrochemical supercapacitors, J. Mater. Chem. 21 (2011) 16216–16222.
[82] M. Sawangphruk, M. Suksomboon, K. Kongsupornsak, J. Khuntilo, P. Srimuk, Y. Sanguansak, P. Klunbud, P. Suktha, P. Chiochan, High-performance supercapacitors based on silver nanoparticle-polyaniline-graphene nanocomposites coated on flexible carbon fiber paper, J. Mater. Chem. A 1 (2013) 9630–9636.
[83] X. Li, C. Zhang, S. Xin, Z. Yang, Y. Li, D. Zhang, P. Yao, Facile synthesis of MoS2/Reduced graphene oxide@polyaniline for high-performance supercapacitors, ACS Appl. Mater. Interfaces 8 (2016) 21373–21380.
[84] K.V. Sankar, R.K. Selvan, The ternary MnFe2O4/graphene/polyaniline hybrid composite as negative electrode for supercapacitors, J. Power Sources 275 (2015) 399–407.
[85] L. Dai, Functionalization of graphene for efficient energy conversion and storage, Acc. Chem. Res. 46 (2012) 31–42.
[86] B. Luo, Y. Fang, B. Wang, J. Zhou, H. Song, L. Zhi, Two dimensional graphene–SnS 2 hybrids with superior rate capability for lithium ion storage, Energy Environ. Sci. 5 (2012) 5226–5230.
[87] B. Luo, B. Wang, X. Li, Y. Jia, M. Liang, L. Zhi, Graphene-confined Sn nanosheets with enhanced lithium storage capability, Adv. Mater. 24 (2012) 3538–3543.
[88] S. Li, D. Wu, C. Cheng, J. Wang, F. Zhang, Y. Su, X. Feng, Polyaniline-coupled multifunctional 2D metal oxide/hydroxide graphene nanohybrids, Angew. Chem. Int. Ed. 52 (2013) 12105–12109.
[89] Y. Xu, Y. Tao, H. Li, C. Zhang, D. Liu, C. Qi, J. Luo, F. Kang, Q.-H. Yang, Dual electronic-ionic conductivity of pseudo-capacitive filler enables high volumetric capacitance from dense graphene micro-particles, Nano Energy 36 (2017) 349–355.
[90] H. Wang, Q. Hao, X. Yang, L. Lu, X. Wang, Effect of graphene oxide on the properties of its composite with polyaniline, ACS Appl. Mater. Interfaces 2 (2010) 821–828.
[91] H.-P. Cong, X.-C. Ren, P. Wang, S.-H. Yu, Flexible graphene-polyaniline composite paper for high-performance supercapacitor, Energy Environ. Sci. 6 (2013) 1185–1191.
[92] Q. Zhang, Y. Li, Y. Feng, W. Feng, Electropolymerization of graphene oxide/polyaniline composite for high-performance supercapacitor, Electrochim. Acta 90 (2013) 95–100.
[93] K. Chi, Z. Zhang, J. Xi, Y. Huang, F. Xiao, S. Wang, Y. Liu, Freestanding graphene paper supported three-dimensional porous graphene-polyaniline nanoconnposite synthesized by inkjet printing and in flexible all-solid-state supercapacitor, ACS Appl. Mater. Interfaces 6 (2014) 16312–16319.
[94] P. Yu, X. Zhao, Z. Huang, Y. Li, Q. Zhang, Free-standing three-dimensional graphene and polyaniline nanowire arrays hybrid foams for high-performance flexible and lightweight supercapacitors, J. Mater. Chem. A 2 (2014) 14413–14420.
[95] S. Giri, D. Ghosh, C.K. Das, Growth of vertically aligned tunable polyaniline on graphene/ZrO2 nanocomposites for supercapacitor energy-storage application, Adv. Funct. Mater. 24 (2014) 1312–1324.
[96] M. Yu, Y. Ma, J. Liu, S. Li, Polyaniline nanocone arrays synthesized on three-dimensional graphene network by electrodeposition for supercapacitor electrodes, Carbon 87 (2015) 98–105.
[97] J. Pedros, A. Bosca, J. Martinez, S. Ruiz-Gomez, L. Perez, V. Barranco, F. Calle, Polyaniline nanofiber sponge filled graphene foam as high gravimetric and volumetric capacitance electrode, J. Power Sources 317 (2016) 35–42.
[98] N. Chen, Y. Ren, P. Kong, L. Tan, H. Feng, Y. Luo, In situ one-pot preparation of reduced graphene oxide/polyaniline composite for high-performance electrochemical capacitors, Appl. Surf. Sci. 392 (2017) 71–79.
[99] P. Yu, X. Zhao, Y. Li, Q. Zhang, Controllable growth of polyaniline nanowire arrays on hierarchical macro/mesoporous graphene foams for high-performance flexible supercapacitors, Appl. Surf. Sci. 393 (2017) 37–45.